

Iridium, Rhodium, and Ruthenium Catalysts for the “Aldehyde–Water Shift” Reaction

Timothy P. Brewster,[§] William C. Ou,[‡] Jeremy C. Tran,[§] Karen I. Goldberg,[§] Susan K. Hanson,[†] Thomas R. Cundari,^{*,‡} and D. Michael Heinekey^{*,§}

[§]Department of Chemistry, University of Washington, Seattle, Washington 98195-1700, United States

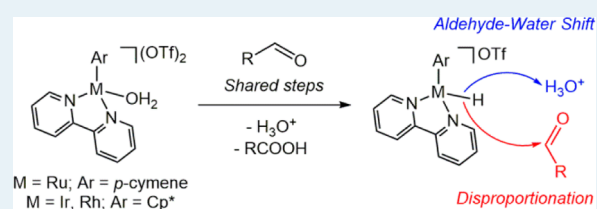
[†]Division of Chemistry, Los Alamos National Laboratory, MS J572, Los Alamos, New Mexico 87545, United States

[‡]Department of Chemistry, Center for Advanced Scientific Computing and Modeling (CASCAM), University of North Texas, P.O. Box 305070, Denton, Texas 76203-5070, United States

Supporting Information

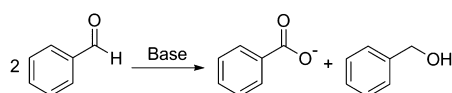
ABSTRACT: A series of half-sandwich complexes of iridium, rhodium, and ruthenium are shown to be active catalysts for the conversion of aldehydes and water to carboxylic acids. Depending on the catalyst, H₂ is either released (the “aldehyde–water shift”) or transferred to a second equivalent of aldehyde (aldehyde disproportionation). Mechanistic studies suggest hydride transfer to be the selectivity-determining step along the reaction pathway. Using [(*p*-cymene)Ru(bpy)OH₂][OTf]₂ as precatalyst, we demonstrate a novel example of a highly selective aldehyde–water shift in the absence of a hydrogen acceptor or base.

KEYWORDS: aldehyde oxidation, homogeneous catalysis, dehydrogenation, disproportionation, water



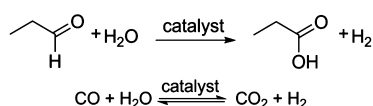
Carboxylic acids are important organic compounds, utilized in a wide variety of consumer products, and serve as synthetic precursors to esters, amides, and polymers. Production of carboxylic acids from aldehydes can be achieved with a wide variety of oxidants, such as permanganate, hydrogen peroxide, and oxygen.¹ Aldehyde disproportionation, in which the aldehyde itself serves as the oxidant, is also well established. In the Cannizzaro reaction, an aldehyde bearing no α -hydrogens undergoes disproportionation under basic conditions to afford a carboxylate salt and a primary alcohol (Scheme 1).¹ Catalysis of aldehyde disproportionation under

Scheme 1. Cannizzaro Reaction



neutral conditions has also been reported by Maitlis using a series of half-sandwich iridium, rhodium, and ruthenium precursors.^{2,3} An intriguing alternative method for generating commercially valuable carboxylic acids from aldehydes is the “aldehyde–water shift” (AWS) reaction,⁴ analogous to the well-studied water–gas shift reaction (Scheme 2), in which water

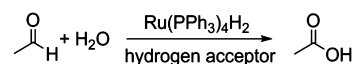
Scheme 2. Aldehyde–Water Shift and Water–Gas Shift



serves as the terminal oxidant. Utilizing this strategy, aldehydes could be oxidized in an atom-economical fashion under mild conditions while also liberating hydrogen gas as a valuable byproduct.

The AWS reaction was first demonstrated in 1987 by Murahashi using a ruthenium catalyst (Scheme 3) in the

Scheme 3. AWS Reported by Murahashi⁵



presence of a hydrogen acceptor as part of a larger study of the conversion of alcohols and aldehydes to esters and lactones.⁵ Much later, Stanley observed carboxylic acids as side products of hydroformylation reactions catalyzed by a dimeric rhodium catalyst and suggested the AWS as a likely reaction pathway.⁴ To the best of our knowledge, these are the only direct demonstrations of the AWS reaction.

The AWS reaction may also play a role in the dehydrogenative oxidation of primary alcohols. Beller^{6–8} and Grützmacher⁹ have independently published reports demonstrating oxidation of aqueous methanol to carbon dioxide with release of three equivalents of H₂. Grützmacher¹⁰ and Milstein¹¹ have shown a more general oxidation reaction in which a wide range of primary alcohols can be oxidized to the corresponding

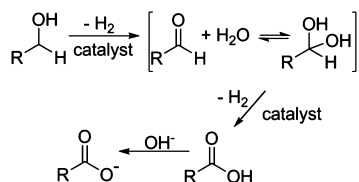
Received: June 17, 2014

Revised: July 24, 2014

Published: July 29, 2014

carboxylate salt in the presence of base. The reactions are thought to follow a reaction pathway similar to that suggested by Milstein in his oxidative esterification and amidation reactions of terminal alcohols and the “oxidant-free” transformation of cyclic amines to lactams.^{12–14} In the rate-limiting step, the alcohol is dehydrogenated to generate an aldehyde, which is in equilibrium with its *gem*-diol.¹¹ The *gem*-diol is then dehydrogenated to generate the carboxylic acid, which is rapidly deprotonated by the added base (Scheme 4).¹⁵

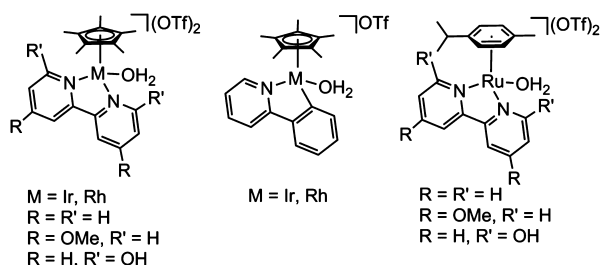
Scheme 4. Acceptorless Alcohol Dehydrogenation Reported by Grützmacher and Milstein.^{10,11}



Here we report a novel example of the AWS reaction in the absence of a hydrogen acceptor or base. The reaction proceeds under neutral aqueous conditions using iridium, rhodium, and ruthenium catalysts. For all catalysts investigated, a competition between the AWS reaction and aldehyde disproportionation was observed. Experimental and computational studies suggest a possible pathway for this reaction.

The AWS reaction is the microscopic reverse of the aqueous hydrogenation of a carboxylic acid. Consequently, we hypothesized that a series of half-sandwich iridium and rhodium complexes recently found to catalyze the hydrogenation of carboxylic acids¹⁶ may also be able to catalyze the AWS reaction. In addition, related complexes are known to be capable of generating H₂ from alcohols under aqueous conditions.¹⁷ Initially, several complexes were evaluated as precatalysts (Chart 1). Dicationic complexes of the form [(*p*-

Chart 1. Catalysts Screened for the AWS Reaction



cymene)Ru(L-L)OH₂][OTf]₂ and [Cp**M*(L-L)OH₂][OTf]₂ (Cp* = 1,2,3,4,5-pentamethylcyclopentadienide, M = Ir, Rh, L-L = 2,2'-bipyridine (bpy), 4,4'-dimethoxy-2,2'-bipyridine (bpy-OMe), 6,6'-dihydroxy-2,2'-bipyridine (bpy-OH), OTf = trifluoromethanesulfonate) were prepared.¹⁸ Monocationic [Cp**M*(ppy)OH₂][OTf] (M = Ir, Rh, ppy = κ -C¹-phenylene-2,2'- κ -N-pyridine) complexes were synthesized by reaction of phenylpyridine with [Cp**M*(OH₂)₃][OTf]₂.¹⁸ For convenience, complexes will hereafter be referred to by the metal and pyridyl ligand (i.e., [Cp*Ir(bpy)OH₂][OTf]₂ = Ir(bpy)).

The Ru, Rh, and Ir complexes were tested for catalytic activity in the AWS reaction utilizing propionaldehyde as a model substrate. In a typical reaction, the catalyst (0.4 mol %) was dissolved in 10 mL of 0.500 M aqueous propionaldehyde

and heated at 105 °C for 20 h in a Teflon-sealed glass reaction vessel. Products and product yields were determined by ¹H NMR spectroscopy utilizing phenol as an internal standard (see Supporting Information). In addition to the desired carboxylic acid product and unreacted starting material (aldehyde and the corresponding *gem*-diol) the corresponding alcohol reduction product resulting from aldehyde disproportionation was observed as the remainder of the converted starting material, as summarized in Table 1.

When using Ir(bpy) or Ru(bpy) as precatalyst, the ¹H NMR spectrum of the product mixture shows resonances corresponding to a coordinated bipyridine ligand. Signals attributable to alkyl groups of coordinated Cp* and *p*-cymene can also be observed when acetaldehyde is utilized as substrate further suggesting that the precatalyst remains intact for the duration of the reaction.¹⁹ However, due to the low catalyst concentration relative to substrate (and the corresponding low signal-to-noise ratio observed for catalyst resonances), it could not be conclusively shown that catalyst decomposition was not occurring. Therefore, homogeneity of the catalysts was further investigated by performing test reactions in the presence of a drop of metallic mercury. In all cases, the addition of mercury did not significantly alter the composition of the final reaction mixture, suggesting that the active catalyst for the reaction is a homogeneous metal complex.

Two metrics were utilized to evaluate the viability of each precatalyst. First, percent conversion of starting material was used to gauge the overall activity of the respective complexes. Second, the reaction rate for the aldehyde–water shift relative to the competing aldehyde disproportionation was inferred from the amount of carboxylic acid present in the converted products.²⁰

The iridium bipyridyl complexes were the most active catalyst precursors, displaying near quantitative conversion of propionaldehyde. The rhodium precatalysts followed a reversed activity trend to that observed from the iridium analogues; Rh(ppy) displayed a high conversion rate when compared to the bpy and bpy-OMe analogues. Surprisingly, precatalysts featuring the bpy-OH ligand, which might be expected to serve as a proton shuttle,^{17,21,22} did not function differently from the electronically similar bpy-OMe complexes which do not possess this potential for bifunctionality.

Ruthenium complexes consistently exhibited slow rates of reaction. Although Maitlis and co-workers did not observe disproportionation utilizing [(C₆Me₆)Ru(OH)₃]Cl·4H₂O in the presence of bpy at 50 °C,³ we observed turnover at 105 °C using the closely related Ru(bpy) catalyst. Moreover, the low conversion measured after 18 h is not a result of catalyst deactivation, as longer reaction times utilizing the Ru(bpy) catalyst lead to further conversion to products. For the Ru catalysts tested, doubling the catalyst loading doubled the percent conversion of starting material, suggesting a first-order rate dependence on the metal (Table 1).

For many of the catalysts tested, propionic acid is present as approximately 50% of the converted product, indicating that disproportionation is the reaction preferentially catalyzed, and there is little AWS occurring. However, the Ir(ppy) and Ru(bpy) precatalysts stand out (Table 1), both demonstrating greater than 70% selectivity for acid production. At 75% selectivity for acid production, two-thirds of the generated acid is derived from the AWS, while one-third results from disproportionation.

Table 1. Precatalyst Screen Results^a

Precatalyst	0.4 mol % Catalyst			0.8 mol % Catalyst		
	Conversion	% Acid	% AWS	Conversion	% Acid	% AWS
Rh(bpy)	16(4)	55(7)	18(20)	28(4)	53(1)	11(4)
Rh(ppy)	95(1)	51(1)	4(4)	95(6)	54(2)	15(8)
Rh(bpy-OMe)	17(3)	60(3)	33(7)	26(2)	56(1)	21(3)
Rh(bpy-OH)	39(3)	54(1)	15(4)	82(1)	51(1)	4(4)
Ir(bpy)	99(1)	52(2)	8(8)	99(1)	54(5)	15(15)
Ir(ppy)	3(1)	73(4)	63(8)	4(2)	73(6)	63(13)
Ir(bpy-OMe)	99(1)	53(3)	11(11)	99(1)	52(2)	8(8)
Ir(bpy-OH)	99(1)	50(1)	0(4)	99(1)	51(1)	4(4)
Ru(bpy)	5(1)	76(5)	68(9)	9(1)	75(5)	67(10)
Ru(bpy-OMe)	5(1)	71(2)	59(4)	9(2)	57(4)	25(14)
Ru(bpy-OH)	6(1)	62(2)	39(6)	12(6)	59(3)	31(10)

^a% Reaction run in 10 mL of aqueous propionaldehyde. % Acid based on converted propionaldehyde. % AWS: percent of acid product obtained from AWS; calculated as (% Acid - (1 - % Acid))/% Acid.²⁰ In parentheses: Standard deviation for "Conversion" and "% Acid." Error in "% AWS" calculated based on 1 standard deviation of % Acid.

To confirm that the carboxylic acid product is produced via the AWS, production of hydrogen was investigated by exposing the headspace gas from a propionaldehyde reaction to a solution of Ir(Cl)(CO)(PPh₃)₂ in benzene.²³ ¹H and ³¹P{¹H} NMR analysis demonstrated the expected formation of Ir(Cl)(CO)(PPh₃)₂(H)₂, confirming the production of hydrogen gas (see Supporting Information for full details).²⁴

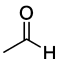
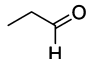
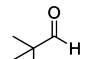
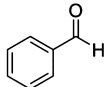
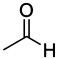
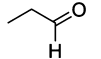
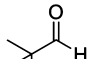
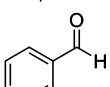
The substrate scope of the reaction was then investigated utilizing active catalyst Ir(bpy) and selective catalyst Ru(bpy) (Table 2). Both catalysts demonstrated essentially identical reactivity with acetaldehyde and propionaldehyde (entries 1 and 2 for Ir(bpy) and 4 and 5 for Ru(bpy)). The more sterically hindered pivaldehyde showed similar selectivity but decreased

activity when compared to propionaldehyde. This may be due to the lower aqueous solubility of pivaldehyde when compared to propionaldehyde (reactions of pivaldehyde were biphasic).

Though the reactivity of benzaldehyde with the Ir(bpy) catalyst is quite similar to that of the other substrates (low conversion is again due to poor substrate solubility), the reactivity of benzaldehyde and water in the presence of Ru(bpy) is markedly different. In this case, the reaction is 95% selective for the production of carboxylic acid over alcohol. Thus, 95% of the generated carboxylic acid can therefore be attributed to AWS reactivity.

Investigation of a plausible AWS mechanism was carried out using DFT. Our working hypotheses for steps in the AWS mechanism are based on proposals for related reactions by Stanley and co-workers,⁴ Maitlis and co-workers,³ Yamaguchi and co-workers,¹⁷ Grützmacher and co-workers,¹⁰ and Milstein and co-workers,¹¹ as well as the DFT studies of aqueous alcohol oxidation reported by Li and Hall.¹⁵ Our mechanism starts with acetaldehyde and model catalyst [Cp*Ir(bpy)]²⁺(A), a 16-electron species with a vacant coordination site. Initial calculations with Ir(I) and Ir(V) entities indicated these to be much higher in free energy, so DFT modeling focused on Ir(III) complexes. The cycle begins with coordination of MeCHO to Ir, forming B. Computations suggest that κ¹-O is the preferred ligation mode (versus κ²-C,O) of the aldehyde substrate in B. Next, as hypothesized by Stanley et al.,⁴ a weak donor-acceptor interaction between H₂O and the carbonyl carbon of the ligated acetaldehyde was sought and found, yielding a minimum, C, termed the hydrate tautomer. Ligation of the two substrates is computed to be mildly endergonic in aqueous solvent model, ΔG_{A→B} = +2 kcal/mol and ΔG_{B→C} = +8 kcal/mol. Hydrate tautomer C may then tautomerize to a "diol" form, D, the latter being lower in energy by 3 kcal/mol and requiring the surmounting of a modest free energy barrier of 14 kcal/mol. Next, in a concerted dehydrogenation, H⁺ and H⁻ are simultaneously transferred to water and the metal, respectively, producing hydronium and hydride complex E. In species E, acetic acid is no longer coordinated to the metal, but is instead stabilized by a hydrogen bond between the acetic acid hydroxyl group and the hydride ligand. Acetic acid may then dissociate from E, forming species F. This step is entropically favored, ΔG_{E→F} = -8 kcal/mol. Finally, H₂ is released from F to close the cycle; this step is computed to be exergonic by 11 kcal/mol. In the competing disproportionation reaction, F

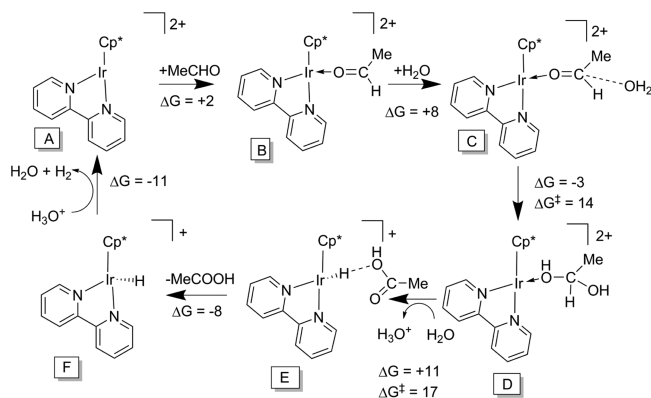
Table 2. Substrate Screen for AWS Reactivity^a

Precatalyst	Substrate	Conversion	% Acid ^b	% AWS ^b
Ir(bpy) ^b		99(1)	54(0.2)	15(1)
		99(1)	52(2)	8(8)
		29(3)	58(2)	27(6)
		16(2)	49(2)	0(4)
Ru(bpy) ^b		7(1)	73(1)	63(2)
		5(1)	76(5)	68(9)
		2(0.3)	75(4)	66(6)
		4(2)	95(4)	95(5)

^a0.4 mol % catalyst in 10 mL H₂O, 5 mmol substrate, 105 °C, 20 h. ^b% Acid based on converted aldehyde. % AWS: percent of acid product obtained from AWS; calculated as (% Acid - (1 - % Acid))/% Acid.²⁰ In parentheses: Standard deviation for "Conversion" and "% Acid." Error in "% AWS" calculated based on 1 standard deviation of % Acid.

transfers the hydride to an additional equivalent of aldehyde as proposed in an analogous hydrogenation mechanism.¹⁶ Thus, though other pathways could be envisioned, all of the steps in Scheme 5 yield an energetically feasible route for the AWS reaction. Full investigation into the mechanism is underway.

Scheme 5. Modeled Mechanism for AWS with Cp*Ir Catalyst^a



^aComputed free energies (kcal/mol) in continuum aqueous solvent are noted.

Observed reactivity trends are consistent with this mechanistic proposal. Dicationic iridium complexes, which form stronger M—H bonds than their rhodium analogues,²⁵ would be expected to react more quickly as hydride formation is calculated to be rate limiting. However, the resultant iridium hydrides are very weak bases,^{26,27} and therefore the reaction favors disproportionation. In an effort to promote the formation of H₂ via protonation of the generated metal hydride (F in Scheme 5), substrates were screened utilizing the Ir(bpy) and Ru(bpy) catalysts in aqueous HBF₄ (1M) (See Supporting Information).²⁸ In all cases, the percent carboxylic acid produced was not observed to increase in the presence of HBF₄. In the case of the slower Ru(bpy) catalyst, substrates bearing α -hydrogens were observed to undergo aldol condensation yielding an immiscible organic layer over the course of the reaction.²⁹

Reaction selectivity observed in the substrate screen is also consistent with our mechanistic hypothesis. Acetaldehyde, propionaldehyde, and pivaldehyde are electronically quite similar and likely will have similar propensity for hydride transfer from the metal center. Benzaldehyde, which is fully conjugated, is less electrophilic, thereby allowing for high selectivity with the Ru(bpy) catalyst. Ir(bpy), whose corresponding hydride is not sufficiently basic to competitively deprotonate water,²⁶ still displays disproportionation behavior. Future studies will focus on the development and utilization of catalysts, which are known to be basic enough to achieve this disproportionation, thereby allowing for high AWS selectivity.²⁷

In conclusion, we have demonstrated the viability of the aldehyde–water shift reaction, an attractive method for the oxidation of aldehydes using water as terminal oxidant. AWS reactivity was found to be in competition with aldehyde disproportionation. High selectivity (95(4)%) for the AWS was achieved when using [(*p*-cymene)Ru(bpy)OH₂][OTf]₂ as precatalyst and benzaldehyde as substrate, a novel example of a selective AWS in the absence of a hydrogen acceptor. Utilization of water as the terminal oxidant in the oxidation of

aldehydes allows this reaction to proceed under exceptionally mild conditions. This represents an exciting addition to the suite of fundamental organic transformations and could have great impact within synthetic organic chemistry. Studies into the development of catalysts that are both highly efficient and highly selective for AWS reactivity are currently underway.

■ ASSOCIATED CONTENT

Supporting Information

Full experimental details, NMR spectra, and computational details. This material is available free of charge via the Internet at <http://pubs.acs.org>.

■ AUTHOR INFORMATION

Corresponding Authors

*E-mail: t@unt.edu (T.R.C.).

*E-mail: heinekey@chem.washington.edu (D.M.H.).

Author Contributions

All authors have given approval to the final version of the manuscript.

Notes

The authors declare no competing financial interest.

■ ACKNOWLEDGMENTS

This work was supported by the Camille and Henry Dreyfus Postdoctoral Program in Environmental Chemistry (T.P.B., K.I.G.), by the Washington NASA Space Grant (J.C.T.), and by NSF under the CCI Center for Enabling New Technologies through Catalysis (CENTC), CHE-1205189 (T.P.B., J.C.T., K.I.G., S.K.H., T.R.C., D.M.H.). W.C.O. is a student in the Texas Academy of Math and Science (TAMS) at the University of North Texas (UNT) and thanks the TAMS Summer Research Fellowship for its support of this research. The authors acknowledge Dr. David L. Thorn for helpful discussions.

■ REFERENCES

- (1) Smith, M. B.; March, J. *March's Advanced Organic Chemistry: Reactions, Mechanisms, and Structure*, 6th ed.; John Wiley and Sons, Inc.: Hoboken, NJ, 2007.
- (2) Cook, J.; Hamlin, J. E.; Nutton, A.; Maitlis, P. M. *J. Chem. Soc., Chem. Commun.* **1980**, 144–145.
- (3) Cook, J.; Hamlin, J. E.; Nutton, A.; Maitlis, P. M. *J. Chem. Soc., Dalton Trans.* **1981**, 2342–2352.
- (4) Stanley, G. G.; Aubry, D. A.; Bridges, N.; Barker, B.; Courtney, B. *Prepr. Pap. - Am. Chem. Soc., Div. Fuel Chem.* **2004**, *49*, 712–713.
- (5) Murahashi, S.-I.; Naota, T.; Ito, K.; Maeda, Y.; Taki, H. *J. Org. Chem.* **1987**, *52*, 4319–4327.
- (6) Nielsen, M.; Alberico, E.; Baumann, W.; Drexler, H.-J.; Junge, H.; Gladiali, S.; Beller, M. *Nature* **2013**, *495*, 85–89.
- (7) Monney, A.; Barsch, E.; Sponholz, P.; Junge, H.; Ludwig, R.; Beller, M. *Chem. Commun.* **2014**, *50*, 707–709.
- (8) Alberico, E.; Sponholz, P.; Cordes, C.; Nielsen, M.; Drexler, H.-J.; Baumann, W.; Junge, H.; Beller, M. *Angew. Chem., Int. Ed.* **2013**, *52*, 14162–14166.
- (9) Rodriguez-Lugo, R. E.; Trincado, M.; Vogt, M.; Tewes, F.; Santiso-Quinones, G.; Grützmacher, H. *Nat. Chem.* **2013**, *5*, 342–347.
- (10) Zweifel, T.; Naubron, J.-V.; Grützmacher, H. *Angew. Chem., Int. Ed.* **2009**, *48*, 559–563.
- (11) Balaraman, E.; Khaskin, E.; Leitun, G.; Milstein, D. *Nat. Chem.* **2013**, *5*, 122–125.
- (12) Zhang, J.; Leitun, G.; Ben-David, Y.; Milstein, D. *J. Am. Chem. Soc.* **2005**, *127*, 10840–10841.
- (13) Gunanathan, C.; Ben-David, Y.; Milstein, D. *Science* **2007**, *317*, 790–792.

- (14) Khusnutdinova, J. R.; Ben-David, Y.; Milstein, D. *J. Am. Chem. Soc.* **2014**, *136*, 2998–3001.
- (15) Li, H.; Hall, M. B. *J. Am. Chem. Soc.* **2014**, *136*, 383–395.
- (16) Brewster, T. P.; Miller, A. J. M.; Heinekey, D. M.; Goldberg, K. I. *J. Am. Chem. Soc.* **2013**, *135*, 16022–16025.
- (17) Kawahara, R.; Fujita, K.-I.; Yamaguchi, R. *J. Am. Chem. Soc.* **2012**, *134*, 3643–3646.
- (18) For synthetic details, see Supporting Information.
- (19) Under analogous conditions, [(*p*-cymene)RuCl₂]₂ rapidly decomposes to heterogeneous material.
- (20) For example, if 4 mmol of aldehyde is converted to products, and 3 mmol (75%) of the observed product is carboxylic acid, 1 mmol of the carboxylic acid product results from disproportionation, and 2 mmol result from AWS.
- (21) Wang, W.-H.; Hull, J. F.; Muckerman, J. T.; Fujita, E.; Himeda, Y. *Energy Environ. Sci.* **2012**, *5*, 7923–7926.
- (22) Nieto, I.; Livings, M. S.; Sacci, J. B., III; Reuther, L. E.; Zeller, M.; Papish, E. T. *Organometallics* **2011**, *30*, 6339–6342.
- (23) For a related example, see Finney, E. E.; Ogawa, K. A.; Boydston, A. J. *J. Am. Chem. Soc.* **2012**, *134*, 12374–12377.
- (24) Burk, M. J.; McGrath, M. P.; Wheeler, R.; Crabtree, R. H. *J. Am. Chem. Soc.* **1988**, *110*, 5034–5039.
- (25) Simoes, J. A. M.; Beauchamp, J. L. *Chem. Rev.* **1990**, *90*, 629–688.
- (26) Vogt, M.; Pons, V.; Heinekey, D. M. *Organometallics* **2005**, *24*, 1832–1836.
- (27) Morris, R. H. *J. Am. Chem. Soc.* **2014**, *136*, 1948–1959.
- (28) Rh(bpy) was also tested utilizing propionaldehyde as substrate. This led to aldol products.
- (29) 31% aldol product was also observed using Ir(bpy) with propionaldehyde as substrate. This was not observed using acetaldehyde in the presence of Ir(bpy).